
Article:
Mehmood, F., Khan, B., Ali, S.M. et al. (1 more author) (2021) Distributed MPC for economic dispatch and intermittence control of renewable based autonomous microgrid. Electric Power Systems Research, 195. 107131. ISSN 0378-7796

https://doi.org/10.1016/j.epsr.2021.107131

Distributed Model Predictive Control for Frequency Regulation and Economic Dispatch of Autonomous Microgrid

Faisal Mehmood, Bilal Khan, Shaibzada Muhammad Ali, John Anthony Rossiter

***Abstract*—This work addresses Autonomous Microgrids composed of Distributed Renewable Energy Sources (DRES). The interconnection of DRES forms a nonlinear system with coupled dynamics, unknown network parameters, and network topologies. The challenging features of DRES, such as: low inertia, large number, volatile production limits, and geographically wide distribution possess critical control design challenges for frequency regulation and Economic Dispatch (ED). Whereas the distributed control schemes proposed in contemporary research are either too slow to provide ED in the presence of fluctuating power demand or too restrictive in terms of network topology to have practical significance. Moreover, the control schemes are unable to handle the production constraints of DRES and lead to instability in the presence of volatile production limits. Considering the above, we propose Secondary Distributed Model Predictive Control providing fast and robust convergence. The control is proposed for generalized network topologies by employing a unique technique of creating a decoupled system. Where each DRES node forms an equivalent model of entire network. The constrained ED solution is derived and successfully achieved with the help of proposed Constrained Handling Algorithm. The Lyapunov stability of control is proved through terminal constraints. The performance of the proposed control is validated using an IEEE 14-Bus System.**

***Index Terms*—Distributed , Distributed Secondary Control, Economic Load Dispatch, Frequency Regulation, Microgrid.**

I. Introduction

The reliance of modern Power Systems on Distributed Renewable Energy Sources (DRES) has increased significantly, reducing fuel-based synchronous generation [1]. The shift from centralized to distributed generation has opened new operating regimes (such as, Microgrid) and control challenges [2]. The centralized control architecture originally designed for bulk generation is inappropriate for a rapidly increasing number of DRES, indicating an essential demand for flexible distributed control with plug and play capabilities [3]. Also, the segmentation of power systems into Microgrids (MG) composed of locally available DRES and storage elements constitutes a low inertia network, specifically during autonomous mode operation [4]. Moreover, the challenging features of DRES, such as: stochasticity, volatile production capacity, and geographically wide distribution, demands a fast-convergent control for frequency regulation and production cost minimization. However, the interconnection of DRES forming an autonomous MG, results in a non-linear system with coupled dynamics [5]. The unknown network parameters and network topology together with fluctuating power demand poses a critical control design challenge. The proposed distributed control solutions in contemporary research works [5],[6],[7] are either too sluggish or based on impractical assumptions. This work proposes a Distributed Model Predictive Control (DMPC) based control solution effectively complying with the control requirements of autonomous MG.

The power produced by DRES is either in the form of DC or high-speed/variable AC, requiring power electronic converters to interface the AC network [8]. Unlike synchronous generators with inherent synchronization capability, the DRES rely on their associated control for synchronization and power sharing [9]. The Figure 1 represents the DRES nodes with associated hierarchal control architecture and internode communication link [10], [11].

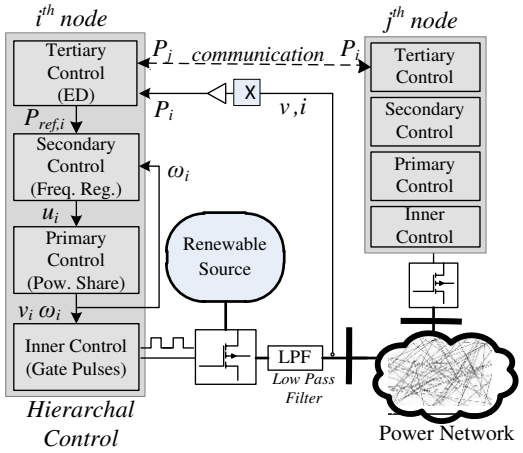

Figure 1. DRES Nodes with Hierarchal Control

In Figure 1, the *inner* control of the inverter works on a faster time scale, providing gate pulses for the converter to produce the voltage of desired amplitude and frequency. The *primary* control is based on a droop control technique to provide the power sharing among the DRES nodes [12], [13]. The *secondary* control provides frequency regulation [14], while the *tertiary* control provides Economic Dispatch (ED) in the system. The modern research works often merge the *tertiary*

control into the *secondary* control, providing the frequency regulation and ED at same level [15]. The *secondary* and *tertiary* control can be centralized [16], as in traditional power system as well as distributed [17], [18]. However, distributed control has gained a lot of interest for an increasing number of DRES. Unlike centralized control requiring direct communication links with individual generating nodes, the distributed control is based on local peer to peer internode communication, thus facilitating plug and play operation [19].

Distributed Averaging Integral (DAI) based distributed control schemes were proposed in contemporary research to provide frequency regulation and proportional power sharing [20]. To reduce the cost of production the criteria for ED was developed in [5],[17] and successfully implemented with DAI. However, such a control possesses sluggish response in a low inertia MG. A Distributed Model Predictive Secondary Control based solution provides active frequency regulation and fast convergence for ED [7]. However, the control is designed on the assumption of known network parameters and is too restrictive in terms of network topology. Moreover, the control deals with the instantaneous phase of local and neighbouring nodes, making the technique difficult to implement.

The above-mentioned contemporary control schemes are unable to handle the production constraints and assume sufficiently large production capacity for each DRES node. This assumption is not practical in the presence of heterogenous DRES with volatile production capacity. Moreover, under stressed network conditions, the violation of the maximum capacity limit would result in system instability.

This paper proposes a Secondary Distributed Model Predictive Control (SDMPC) for frequency regulation and ED. The control overcomes the performance limitations of Distributed Model Predictive Secondary Control [7] and is proposed for a generalized network topology with unknown parameters. The control provides fast convergence and a mechanism to ensure consensus in the network in the presence of the production limitations of DRES.

The foremost challenge in the design of the control scheme is to construct the state predictions in the presence of unknown parameters and coupled dynamics. For this purpose, each DRES node is assumed to be connected exclusively to a virtual-node through a known virtual admittance, thus creating an equivalent of the entire network. The resulting equivalent model possesses decoupled dynamics with known parameters. The idea of a virtual-node is similar to the concept of an infinite-bus in the power system. However, in contrast to an infinite-bus, the phase of the virtual-node is updated in each iteration.

The global equilibrium point of the network is based on frequency regulation and consensus to ED criteria. Moreover, the consensus point varies with fluctuations in the power demand in the system. So, to achieve fast convergence of the proposed control, this paper adopts a novel method for constructing the state errors. Unlike contemporary research works that use the Laplacian Matrix to construct the state error [6], [7], the proposed method is based on preserving the sum of power injections among the neighbouring nodes providing asymptotic convergence to a global equilibrium. The state errors are formed based on local and neighbouring nodes' power injections, using the virtual-node as a reference. The proposed solution also provides a mechanism to handle the production constraints, since restricting the power injection in the optimisation problem results in an infeasible ED problem. The solution is devised by slightly manipulating the value of injected power before communicating to the neighbouring nodes. The major contributions of the paper are highlighted below.

- The DMPC based *secondary* control for autonomous MG is proposed in this paper, that provides frequency regulation and fast convergence to ED-point in presence of fluctuating power demand. The control is proposed for generic network topologies with nonlinear coupled dynamics and unknown network admittance.
- The paper introduces a decoupling technique that creates an equivalent of the network at each power-node. The technique overcomes the problem of unknown parameter and enables the construction of state predictions.
- Considering a practical scenario of volatile power production limits of DRES, a constraint ED solution is derived. The Constraint Handling Algorithm is proposed to achieve the solution and overcome the infeasibility problem.
- The stability of proposed control is achieved using equality based terminal constraints and using the total cost of network as Lyapunov Candidate Function. The performance of the proposed control is validated on an IEEE-14 Bus Test System and the results are compared with DAI control.

The rest of the paper is organised as follows, Section II starts with the introduction of various notations used in the paper, graph theory and modelling of a power network. This Section also presents the control objectives and discusses the DAI and Distributed Model Predictive Secondary Control techniques. Section III presents the design of the proposed Secondary Distributed Model Predictive Control (SDMPC) techniques and constraints handling algorithm. The stability of the proposed control and the convergence of the total cost of the network is proved in Section IV. The simulation results are discussed in Section V.

II. MICROGRID MODELLING

This Section presents the *primary* control dynamics and defines the control objectives for *secondary* control. The solution of the ED problem is derived in the presence of production constraints. The existing distributed *secondary* control techniques and their performance limitations are also discussed. The Section starts with a brief introduction of graph theory and various notations used in the paper.

A. Notations

Let, $\mathbb{R}$ represent the set of real numbers, $\mathbb{R}_{>k}$ is the set $\{x \in \mathbb{R} | x > k\}$, $\mathbb{R}_{\geq k}$ is $\{x \in \mathbb{R} | x \geq k\}$ (where k is an integer) and $\mathbb{O}$ is the null set. The operator $|\cdot|$ represents the cardinality of a set, $col(\cdot)$ creates a column vector from a set, while $\mathfrak{D}(\cdot)$ creates the corresponding diagonal matrix from a set

or column vector provided as argument. $\mathbb{1}_n \in \mathbb{R}^{n\times 1}$ represents the column vector of ones, $\mathbb{0}_n \in \mathbb{R}^{n\times 1}$ represents the column vector of zeros and $I_n \in \mathbb{R}^{n\times n}$ is the identity matrix.

B. Graph Theory

$\mathbb{G}$ is an undirected, static and connected graph consisting of n nodes, represented by the set $N = \{n_1, \dots n_n\}$. The topology of $\mathbb{G}$ is represented by symmetric adjacency matrix $A \in \mathbb{R}_{\geq 0}^{n\times n}$, with elements $a_{ij} = 1$, when the nodes n_i and n_j are connected by an edge, while $a_{ij} = 0$ otherwise. The set of neighbouring nodes of the i^{th} node is defined as; $N_i \coloneqq \{n_j | a_{ij} = 1, j \in N\}$. $\mathbb{Q} \coloneqq \mathfrak{D}(A\mathbb{1}_n)$ is the degree matrix and $\mathcal{L} \coloneqq \mathbb{Q} - A, \in \mathbb{R}^{n\times n}$ is the corresponding Laplacian matrix.

C. Power Network

We represent the autonomous MG with a graph $\mathbb{G}$, consisting of $N = \{n_1, \dots n_n\}$ set of nodes. The nodes in $\mathbb{G}$ are connected through the power lines with impedance $z_{ij} = {}^1\!/_{y_{ij}}$, $i, j \in N$ (here, y_{ij} represents the admittance while, the angle of impedance is represented by $\theta_{z,ij}$). For an i^{th} node, the set of neighbouring nodes, in terms of power links is defined as; $N_{y,i} \coloneqq \{n_j | y_{ij} \neq 0, j \in N\}$. The nodes in $\mathbb{G}$ are either categorized as power-nodes, represented by the set N_P, or passive-nodes N_R ($N_R = N - N_P$). The power-nodes contain a DRES with an optional local-load while, the passive-nodes only contain the (optional) local-load. The power-nodes (N_P) are also connected through communication lines, forming a connected sub-graph in $\mathbb{G}$, with corresponding adjacency matrix $A = [a_{ij}] \in \mathbb{R}_{\geq 0}^{n_P\times n_P}$, the degree and Laplacian matrix $\mathbb{Q} \in \mathbb{R}_{>0}^{n_P\times n_P}$ and $\mathcal{L} \in \mathbb{R}^{n_P\times n_P}$ respectively. The set of neighbouring communication nodes of the i^{th} power-node is defined as; $N_{c,i} \coloneqq \{n_j | a_{ij} = 1, j \in N_P\}$.

Assumption: The focus of presented work is frequency regulation and ED so, for simplicity, the voltage amplitude at each power-node is assumed to be constant: $1\ per\ unit\ (pu)$.

We use second order dynamics for inverter-interfaced DRES to emulate the dynamics of a synchronous generator [5], [21]. The discretized dynamics of a power-node are given below.

$$\theta_i(t+1) = \theta_i(t) + \omega_i(t)\Delta t, \tag{1a}$$

$$\omega_i(t+1) = \omega_i(t) + \frac{\Delta t}{m_i}[-d_i(\omega_i(t) - \omega_d) - p_i(t) + u_i(t)]. \tag{1b}$$

where, $\theta_i \in \mathbb{R}$ and $\omega_i \in \mathbb{R}$ are the phase and angular frequency of the power-node respectively, $m_i \in \mathbb{R}_{>0}$ is the virtual inertia, $d_i \in \mathbb{R}_{>0}$ is damping factor, $\omega_d \in \mathbb{R}_{>0}$ is the desired angular frequency and $u_i \in \mathbb{R}$ is the control input from *secondary* control. The discrete time is represented by t and Δt represents the time-step. The power injection of the power-node is represented by $p_i \in \mathbb{R}$, which is the sum of power absorbed by the local-load $(p_{LL,i} \in \mathbb{R})$ and power delivered to the neighbouring nodes $(p_{n,i} \in \mathbb{R})$.

$$p_i(t) = p_{LL,i}(t) + p_{n,i}(t). \tag{2}$$

Here, $p_{n,i}$ is the sinusoidal function of phase angle, voltage magnitude (of both the local and neighbouring nodes) and admittance of the power line.

$$p_{n,i}(t) = \sum_{j\in N_{y,i}} y_{ij} \begin{pmatrix} {v_i}^2 \cos(\theta_{z,ij}) - \\ v_i v_j \cos\left(\theta_{z,ij} + \theta_i(t) - \theta_j(t)\right) \end{pmatrix}. \tag{3}$$

However, in case of a lossless power line, (3) reduces to,

$$p_{n,i}(t) = \sum_{j\in N_{y,i}} b_{ij} v_i v_j \sin\left(\theta_i(t) - \theta_j(t)\right). \tag{4}$$

Here, v_i represents the voltage of i^{th} power-node and b_{ij} is the inter-node susceptance. We define the deviation state-variables as, $\Delta\omega_i(t) = \omega_i(t) - \omega_d$ and $\Delta\theta_i(t) = \theta_i(t) - \theta_d(t)$, with $\theta_d(t) = t\omega_d\Delta t$. So, (1) can be rewritten in terms of deviation variables as,

$$\Delta\theta_i(t+1) = \Delta\theta_i(t) + \Delta\omega_i(t)\Delta t, \tag{5a}$$

$$\Delta\omega_i(t+1) = \Delta\omega_i(t) + \frac{\Delta t}{m_i}\big[-d_i\Delta\omega_i(t) - p_{LL,i}(t) - p_{n,i}(t) + u_i(t)\big]. \tag{5b}$$

While, the dynamics of passive-nodes are given by:

$$p_{n,i}(t) = -p_{LL,i}(t). \tag{6}$$

In (5), the control input (u_i) is provided by the *secondary* control to regulate the frequency and achieve the ED in the system.

Lemma 1: The system represented in eqns. (5) and (6) under constant control input $\bar{u} \in \mathbb{R}^{n_P\times 1}$ $(u(t) = col(u_i) = \bar{u} \in \mathbb{R}^{n_P\times 1})$, results in constant synchronous frequency $\omega_s \in \mathbb{R}$ $\big(\omega(t) = col(\omega_i) = \omega_s\mathbb{1}_{n_P}\big)$, which does not necessarily equal the desired frequency ω_d.

The proof of the Lemma is present in [5],[6]. The summation of (5b) over the entire set of power-nodes with constant frequency $\omega(t) = \omega_s\mathbb{1}_{n_P}$ results in:

$$0 = \mathbb{1}_{n_P}^T\big[-D(\omega_s - \omega_d)\mathbb{1}_{n_P} - P + \bar{u}\big],$$

$$\omega_s = \omega_d + \frac{-\mathbb{1}_{n_P}^T P + \mathbb{1}_{n_P}^T\bar{u}}{\mathbb{1}_{n_P}^T D\mathbb{1}_{n_P}}. \tag{7}$$

Here, $D = \mathfrak{D}(d_i) \in \mathbb{R}^{n_P\times n_P}$ and $P = col(p_i) \in \mathbb{R}^{n_P\times 1}$. The sum of power produced $\big(\mathbb{1}_{n_P}^T P\big)$ at the power-nodes is equal to the sum of power consumed; $\mathbb{1}_n^T L$ $\big(L \coloneqq col(p_{LL,i}) \in \mathbb{R}_{\geq 0}^{n\times n}\big)$ and power loss P_{loss} in the network, so (7) becomes:

$$\omega_s = \omega_d + \frac{-\mathbb{1}_n^T L - P_{loss} + \mathbb{1}_{n_P}^T\bar{u}}{\mathbb{1}_{n_P}^T D\mathbb{1}_{n_P}}. \tag{8}$$

Equation (8) together with (5b) implies that frequency regulation ($\Delta\omega = 0$ or $\omega(t) = \omega_s\mathbb{1}_{n_P} = \omega_d\mathbb{1}_{n_P}$) would be achieved when the control input (u) from *secondary* control would satisfy: $\mathbb{1}_{n_P}^T u = \mathbb{1}_{n_P}^T P = \mathbb{1}_n^T L + P_{loss}$; also for individual power-nodes $u_i = p_i$, $\forall i \in N_P$. Equation (8) clearly indicates that for frequency regulation the *secondary* control is required to be fast enough to cater for the frequent variations in power demand (L).

In addition to frequency regulation, the *secondary* control is also required to provide the ED in the system. Since the power demand in the system (L) varies frequently, the fast convergence of *secondary* control is inevitable.

D. Unconstrained Control Objectives

The control objectives for the *secondary* control are to regulate the frequency and provide the ED based on identical incremental cost criteria [6].

i. $\Delta\omega_i = 0,\ \forall i \in N_P$ (9)

ii. $\sum_{j\in N_P}\left(c_i p_i(t) - c_j p_j(t)\right) = 0,\ \forall i \in N_P.$ (10)

where, $c_i \in \mathbb{R}_{>1}$ represents the production cost rate or the selling cost rate of i^{th} power-nodes. The control objective in (9) represents the frequency regulation, while (10) is the identical incremental cost criteria for production cost minimization (ED). Since the power-nodes also form a connected sub-graph in $\mathbb{G}$ through communication link, the control objective in (10) can also be represented using Laplacian matrix, so (9) and (10) can be rewritten as [5],

$$\Delta\omega = \mathbb{0}_{n_P}, \tag{11}$$

$$\mathcal{L}CP = \mathbb{0}_{n_P}. \tag{12}$$

Here, $C = \mathfrak{D}(c_i) \in \mathbb{R}_{>1}^{n_P \times n_P}$. Now writing (9) and (10) for the equilibrium point;

$$\Delta\omega_i^* = 0, \tag{13}$$

$$c_1 p_1^* = c_2 p_2^* = \cdots = c_{n_P} p_{n_P}^* = \delta^*. \tag{14}$$

where, $\delta^* \in \mathbb{R}_{>0}$ represents the optimum power (incremental) cost for the power-nodes. The optimum cost (δ^*) depends on the production cost rate (c_i) and total power demand (L) in the network (Lemma 1). Equation (13) and (14) can be represented in matrix form as; $\Delta\omega^* = \mathbb{0}_{n_P}$ and $CP^* = \delta^* \mathbb{1}_{n_P}$.

E. Production Constraints

The control solutions in (13) and (14) represent an unconstrained scenario, with no restriction on the power production (p_i) of individual DRES. Considering the variable power production capacities of DRES, the production constraints for the control objectives in (9) and (10) are:

$$P^{min} \leq P \leq P^{max}. \tag{15}$$

Here, $P^{min} = col\left(p_i^{min}\right) \in \mathbb{R}^{n_P \times 1}$ and $P^{max} = col(p_i^{max}) \in \mathbb{R}^{n_P \times 1}$, where p_i^{min} and p_i^{max} represent the minimum and maximum power injection limits of the i^{th} power-node. To represent the solution in the presence of production limits in (15), let (α), (β) and (γ) be the mutually exclusive subsets of power-nodes such that $(\alpha) \cup (\beta) \cup (\gamma) = N_P$. Now the optimum power injection can be represented as:

$$P^* = \begin{bmatrix} \tilde{\mathcal{P}}_{(\alpha)}^{min} & \tilde{\mathcal{P}}_{(\beta)}^{*} & \tilde{\mathcal{P}}_{(\gamma)}^{max}, \end{bmatrix}^T. \tag{16}$$

Where, $\tilde{\mathcal{P}}_{(\beta)}^{*} \in \mathbb{R}_{>0}^{|(\beta)|\times 1}$, satisfies;

$$\tilde{C}\tilde{\mathcal{P}}_{(\beta)}^{*} = \tilde{\delta}^* \mathbb{1}_{|(\beta)|}. \tag{17}$$

Here, $\tilde{C} = \mathfrak{D}(c_i) \in \mathbb{R}_{>0}^{|(\beta)|\times|(\beta)|}$, $i \in (\beta)$ and $\tilde{\delta}^* \in \mathbb{R}$ is the constrained optimum (incremental) cost.

Remark 1: It is intuitively obvious that unconstrained optimum cost (δ^*) is less than (or equal to) the constrained optimum cost $\left(\tilde{\delta}^*\right)$; $\delta^* \leq \tilde{\delta}^*$.

The contemporary distributed *secondary* control solutions are designed to provide only the unconstrained solution defined in (13) and (14). The following sub-sections provide a brief introduction to existing control solutions and their performance limitations.

F. Distributed Averaging Integral

DAI based *secondary* control is designed by integrating the errors in (11) and (12) [5], [6]:

$$u(t+1) = u(t) - \Delta t k_w\,(\Delta\omega) - \Delta t k_p \mathcal{L}Cu. \tag{18}$$

where, k_w and k_p are the weights on errors in frequency and incremental cost respectively. The control in (18) provides active frequency regulation but possesses slow response in creating consensus for ED.

G. Distributed Model Predictive Secondary Control

The Distributed Model Predictive Secondary Control scheme proposed in [7] is based on tracking the desired state values in each iteration. The control provides fast convergence as compared to a DAI technique however, the control has several limitations. First, the calculation of desired state values involves instantaneous phase information of neighbouring nodes, which is difficult to implement practically. Secondly, the control assumes a (constant) known value of power lines' admittance. The calculation of desired states also requires at least a single power line directly connecting the individual power-node to its neighbouring power-nodes, thereby restricting a generalized topology of the network. The desired value of phase deviations are obtained from the Laplacian based error, $\mathcal{L}CP(t) = \mathbb{0}_{n_P}$ (or $\mathbb{Q}CP(t) - ACP(t) = \mathbb{0}_{n_P}$):

$$\acute{P}^*(t+1) = KP(t). \tag{19}$$

where, $K = \mathbb{Q}^{-1}C^{-1}AC$, with multiple eigenvalues on the unit circle, while $\acute{P}^*$ is the intermediate optimum power point. $\acute{P}^*$ is further used in (4) to obtain the desired phase value while, assuming a known value of susceptance b_{ij}, $i, j \in N_P$.

In summary, the contemporary distributed secondary control solutions are unable to achieve the constrained ED solution defined in (16) and (17). Moreover, these control schemes have few limitations: the DAI based control possesses slow response against fluctuating power demand while, the Distributed Model Predictive Secondary Control is based on impractical assumptions. To overcome the above-mentioned performance limitations, the design of appropriate control schemes is proposed and presented in the following Section.

III. Secondary Distributed Model Predictive Control

This work proposes the Secondary Distributed Model Predictive Control (SDMPC) for frequency regulation and ED of autonomous microgrid with the capability to handle the production constraints. The control is proposed for a generalized network topology with unknown network parameters.

The design of SDMPC is based on decoupled *primary* control dynamics of power-nodes. An improved method for calculation of desired state values is adopted providing fast convergence and minimal frequency deviation. The local optimization problem is designed to track the desired state values, with terminal constraints to ensure the stability of the control. The Constraints Handling Algorithm is also proposed to achieve the constrained ED solution in (16) and (17).

A. Decoupled Dynamics & Desired State Values

The unknown values of inter-node power lines' admittance restrict the construction of state predictions for a DMPC architecture. To eliminate the problem of unknown parameters and coupled dynamics, we create an equivalent of the entire network at each power-node. The equivalent of the network is represented by a virtual-node $\left(n_{v,i}\right)$ with constant voltage

$(v_v = 1pu)$ and connected to individual power-nodes through a virtual susceptance (b_v).

Remark 2: The concept of a virtual-node is similar to the concept of an 'infinite-bus', frequently used in power systems. However, unlike an 'infinite-bus' the phase of a virtual-node is adjusted in each iteration, based on power injection (p_i) of the respective power-node. The total power injection of a power-node is assumed to flow towards the virtual-node, thus creating a decoupled non-linear system.

$$p_i(t) = b_v v_i v_v \sin\left(\Delta\theta_i(t) - \Delta\theta_{v,i}(t)\right). \tag{20}$$

The value of b_v and v_v is kept same for all the power-nodes. Now, the phase of virtual-node $\left(\Delta\theta_{v,i}\right)$ can be calculated as:

$$\Delta\theta_{v,i}(t) = \Delta\theta_i(t) - \sin^{-1}\left(\frac{p_i(t)}{v_i v_v b_v}\right). \tag{21}$$

Now, let the variables $\Delta\theta_i$, $\Delta\omega_i$ and p_i be collectively represented as, $\chi_i(t) = [\Delta\theta_i(t) \quad \Delta\omega_i(t) \quad p_i(t)]^T$. So, the system dynamics in (5) and (20) can be compactly represented as:

$$\begin{aligned}\chi_i(t+1) &= f\left(\chi_i(t), \Delta\theta_{v,i}(t), u_i(t)\right),\\ &= \Upsilon\chi_i(t) + \begin{bmatrix} \Delta t\Delta\omega_i(t) \\ \frac{\Delta t}{m_i}\left(-d_i\Delta\omega_i(t) - p_i(t) + u_i(t)\right) \\ b_v v_i v_v \sin\left(\Delta\theta_i(t+1) - \Delta\theta_{v,i}(t)\right)\end{bmatrix}.\end{aligned} \tag{22}$$

where, $\Upsilon = \mathfrak{D}([1 \quad 1 \quad 0])$. To reach the equilibrium state defined in (9) and (10), we compute the values of desired power injection $\left(p_i^d\right)$ and phase deviation $\left(\Delta\theta_i^d\right)$ at each iteration of SDMPC algorithm. Tracking the desired values would lead to a global equilibrium point (the proof is discussed in Section IV). Unlike [7], p_i^d is derived while preserving the sum of power injections of the neighbouring power-nodes $\left(N_{c,i}\right)$, resulting in minimal frequency deviation.

$$p_i^d(t) + \sum_{j\in N_{c,i}} p_j(t) = p_i(t) + \sum_{j\in N_{c,i}} p_j(t). \tag{23}$$

Here, the righthand side represents the measured values of local and neighbouring nodes power injection. Now, the left-hand side can be rewritten using (14):

$$p_i^d(t) + \sum_{j\in N_{c,i}} \frac{c_i}{c_j} p_i^d(t) = p_i(t) + \sum_{j\in N_{c,i}} p_j(t), \tag{24}$$

$$p_i^d(t) = \frac{1}{1 + c_i \sum_{j\in N_{c,i}} 1/c_j}\left(p_i(t) + \sum_{j\in N_{c,i}} p_j(t)\right), \tag{25}$$

from (20),

$$\Delta\theta_i^d(t) = \theta_{v,i} + \sin^{-1}\left(p_i^d(t) b_v / v_i v_v\right). \tag{26}$$

Equation (25) and (26) respectively provide the desired values of power and phase for individual power nodes. The power injection of neighbouring power nodes $\left(p_j\right)$ are obtained using internode communication links. Unlike [7], the desired phase obtained in (26) does not involve the neighbouring nodes phase information.

Note that the value of desired power obtained in (25) represents the unconstrained scenario. The equation would fail to converge in a constrained scenario as it strives to achieve the consensus $CP^* = \delta^* \mathbb{1}_{n_P}$ instead of $\tilde{C}\tilde{\mathcal{P}}^* = \tilde{\delta}^* \mathbb{1}_{\tilde{n}_P}$.

To satisfy the production constraints a Constraint Handling Algorithm is proposed that provides the constrained desired power $\left(\tilde{p}_i^d\right)$ and correction factor (ε_i). The correction factor (ε_i) is used to modify the power trajectories before communicating to neighbouring power-nodes.

B. Local Optimization Problem

The local control of power-nodes is designed to track the desired values. The desired value of phase $\left(\Delta\theta_i^d\right)$ is defined in (26) while, the desired value of frequency is; $\Delta\omega_i^d(t) = 0$. Three different types of trajectories are used in the SDMPC Algorithm. The predicted trajectories $\left(\chi_i^p, u_i^p\right)$ are used in the optimization problem, the optimum trajectories $\left(\chi_i^{op}, u_i^{op}\right)$ are obtained after solving the optimization problem while, the assumed trajectories $\left(\chi_i^a, u_i^a\right)$ are communicated to neighbouring nodes for the calculation of desired states. The actual or implemented values are represented by: χ_i, u_i. The length of prediction horizon $\left(\mathcal{N}_p\right)$ is kept the same for all the nodes. The designed optimisation problem is given below:

The Optimisation Problem $\mathbb{F}_i$*:*

$$\begin{aligned}&min.\ J_i\left(\chi_i^p(:|t), u_i^p(:|t), \chi_i^a(:|t), \Delta\theta_i^d(:|t)\right),\\ &Subj.to\\ &\chi_i^p(0|t) = \chi_i^a(0|t),\\ &\chi_i^p(k+1|t) = f\left(\chi_i^p(k|t), \Delta\theta_{v,i}(t), u_i^p(k|t)\right),\\ &\quad \text{for } k = 0,1,\dots,\mathcal{N}_p - 1,\\ &u_i^p(:|t) \in U,\\ &p_i^p\left(\mathcal{N}_p|t\right) = p_i^d\left(\mathcal{N}_p|t\right), \qquad (27)\\ &\Delta\omega_i^p\left(\mathcal{N}_p|t\right) = 0. \qquad (28)\end{aligned}$$

Where,

$$\begin{aligned}&J_i\left(\chi_i^p(:|t), u_i^p(:|t), \chi_i^a(:|t), \Delta\theta_i^d(:|t)\right)\\ &= \sum_{k=1}^{\mathcal{N}_p} l_i\left(\chi_i^p(:|t), u_i^p(:|t), \chi_i^a(:|t), \Delta\theta_i^d(:|t)\right),\\ &= \sum_{k=1}^{\mathcal{N}_p} ||\chi_i^p(k|t) - \chi_i^a(k|t)||_Q + ||\Delta\theta_i^p(k|t) -\\ &\qquad \Delta\theta_i^d(k|t)||_S + ||\Delta\omega_i^p(k|t)||_T. \qquad (29)\end{aligned}$$

The terminal constraints (27) and (28) are used to force the trajectories to reach the desired states at the end of the prediction horizon. The cost function in (29) penalizes the deviation between predicted and assumed trajectories and the deviation from the desired state values. The weights on errors: $Q \in \mathbb{R}_{>0}^{3\times3}$, $S \in \mathbb{R}_{>0}$ and $T \in \mathbb{R}_{>0}$ serve as the tuning parameters.

C. SDMPC Algorithm $\mathbb{A}_{SDMPC}$*:*

The SDMPC Algorithm consists of the following steps;

Initialization

i. Obtain the initial values of $\chi_i^a(0|0) = \chi_i(0)$ and initialize $u_i^a(0|0) = u_{o,i}$.
ii. Compute the phase of the virtual-node based on initial power injection $\left(p_i(0)\right)$:
$$\Delta\theta_{v,i}(0) = \Delta\theta_i^a(0|0) - \sin^{-1}\left(\frac{p_i(0)}{v_i v_v b_v}\right).$$
iii. Construct the trajectories $\chi_i^a(:|0)$ over the prediction horizon:
$$\chi_i^a(k+1|0) = f\left(\chi_i^a(k|0), \Delta\theta_{v,i}(0), u_i^a(k|0)\right),$$
for $k = 0,1,\dots,\mathcal{N}_p - 1$.

iv. Communicate the power trajectories $p_i^a(:|0)$ to neighbouring nodes.

SDMPC Iterations

1. Compute the desired power and phase:
$$p_i^d(:|t) = \frac{1}{1+c_i \sum_{j\in N_{c,i}} {}^1/_{c_j}} \left(p_i^a(:|t) + \sum_{j\in N_{c,i}} p_j^a(:|t)\right). \quad (30)$$
2. Run the Constraint Handling Algorithm routine ($\mathbb{A}_{\mathbb{C}}$) to obtain the constrained desired power and correction factor:
$$\left(\tilde{p}_i^d(:|t), \varepsilon_i(:|t)\right) = \mathbb{A}_{\mathbb{C}}\left(p_i^d(:|t), p_i^{max}, p_i^{min}\right).$$
3. Find the desired value of phase deviation:
$$\Delta\theta_i^d(:|t) = \theta_{v,i}(t) + \sin^{-1}\left(\tilde{p}_i^d(:|t) b_v / v_i v_v\right). \quad (31)$$
4. Solve the optimal control problem $\mathbb{F}_i$ for optimum control input $\left(u_i^{op}(:|t)\right)$.
5. Compute the optimal trajectories:
$$\chi_i^{op}(0|t) = \chi_i(t-1),$$
$$\chi_i^{op}(k+1|t) = f\left(\chi_i^{op}(k|t), \Delta\theta_{v,i}(t), u_i^{op}(k|t)\right), \quad (32)$$
for $k = 0,1,\dots,\mathcal{N}_p - 1$.
6. Implement the first value of optimum control input $\left(u_i(t) = u_i^{op}(0|t)\right)$ to update the actual states $\left(\chi_i(t)\right)$ in (22).
7. Update the phase of virtual-node:
$$\Delta\theta_{v,i}(t+1) = \Delta\theta_i^{op}(1|t) - \sin^{-1}\left(\frac{p_i(t)}{v_i v_{v,i} b_v}\right). \quad (33)$$
8. Compute the assumed input by one step shifting the optimum control input:
$$u_i^a(k|t+1) = u_i^{op}(k+1|t), \quad (34)$$
for $k = 0,1,\dots,\mathcal{N}_p - 2$,
$$u_i^a(\mathcal{N}_p - 1|t+1) = p_i^{op}(\mathcal{N}_p|t). \quad (35)$$
9. The assumed trajectories are computed based on updated value of $\left(\Delta\theta_{v,i}(t+1)\right)$:
$$\chi_i^a(0|t+1) = \chi_i^{op}(1|t),$$
$$\chi_i^a(k+1|t+1) = f\begin{pmatrix}\chi_i^a(k|t+1), \Delta\theta_{v,i}(t+1),\\ u_i^a(k|t+1)\end{pmatrix}, \quad (36)$$
for $k = 0,1,\dots,\mathcal{N}_p - 1$.
10. Perform the power adjustment of assumed power:
$$p_i^a(k|t+1) = p_i^a(k|t+1) + \varepsilon_i(k|t).$$
11. Communicate the assumed power $\left(p_i^a(:|t+1)\right)$ and production cost rate $\left(c(:|t+1)\right)$ to neighbouring nodes.
12. Increment the time; $t = t+1$.
13. Go to step No. 1.

Here, $u_{o,i}$ represents the initial value of the control input. The Algorithm solves the optimisation problem $\mathbb{F}_i$ in Step No. 4 to obtain the optimum control input, which is used in Step No. 5 to form the optimum trajectories. Step No 6, implements the first value of optimum control input. The virtual phase value is updated based on instantaneous power injection in Step No. 7. The assumed trajectories are formed based on updated values of virtual phase. Equation (35) maintains the terminal state achieved in (27) and (28). The assumed power trajectories are modified using the correction factor in Step No 10. The local and neighbouring assumed power is used in Step No. 1 to compute the desired power while Step No. 2 provides the constrained desired power and correction factor using the following algorithm $\mathbb{A}_{\mathbb{C}}$.

D. Constraint Handling Algorithm $\mathbb{A}_{\mathbb{C}}$:

1. Check whether the desired power is within the production limits,
$if\ p_i^d(k|t) \in [p_i^{min} \quad p_i^{max}]$,
$\tilde{p}_i^d(k|t) = p_i^d(k|t)$,
$\varepsilon_i(k|t) = 0$.
2. If desired power is less than minimum production limit $\left(p_i^d(k|t) < p_i^{min}\right)$ then,
$\tilde{p}_i^d(k|t) = p_i^{min}$,
$\varepsilon_i(k|t) = p_i^d(k|t) - p_i^{min}$.
3. If desired power is greater than maximum production limit $\left(p_i^d(k|t) > p_i^{max}\right)$ then,
$\tilde{p}_i^d(k|t) = p_i^{max}$,
$\varepsilon_i(k|t) = p_i^d(k|t) - p_i^{max}$.

The algorithm $\mathbb{A}_{\mathbb{C}}$ forces the constrained desired power to lie within the production limits: $\tilde{p}_i^d \in [p_i^{min} \quad p_i^{max}]$, resulting in steady state value $u^* = P^* = \tilde{P}^d \in [P^{min} \quad P^{max}]$ and reaching the equilibrium state defined in (16). The algorithm $\mathbb{A}_{\mathbb{C}}$ also provides the correction factor ε_i, which is used in Step No. 10 to modify the assumed power before communicating to neighbouring nodes. As a result, the restriction of local power injection to its production limits is invisible to neighbouring nodes, allowing the rest of the nodes to converge to an optimum production point and satisfy, $\mathcal{L}CP^a = \mathbb{0}_{n_P}$.

Remark 3: The Algorithm $\mathbb{A}_{\text{SDMPC}}$ together with $\mathbb{A}_{\mathbb{C}}$ forces the assumed power (P^a) to converge to identical incremental cost: $CP^a = \tilde{\delta}^* \mathbb{1}_{n_P}$ where, $\tilde{\delta}^*$ represents the constrained optimum cost defined in (17). While the equilibrium point in terms of actual power (P) will be same as defined in (16).

Remark 4: Instead of adopting the standard procedure of handling the constraints in optimization problem $\mathbb{F}_i$, the production constraints are handled in algorithm $\mathbb{A}_{\text{SDMPC}}$ and $\mathbb{A}_{\mathbb{C}}$. The reason lies in divergence of (25) for the constrained equilibrium states in (16). Now, to illustrate the divergence, consider the system in equilibrium state defined in (16). Now, for the system to remain in equilibrium: $p_i^d(t+1) = p_i^d(t) = p_i^*$. However, the desired state for the next iteration using (25) are given by:
$$p_i^d(t+1) = \frac{1}{1+c_i \sum_{j\in N_{c,i}} {}^1/_{c_j}} \left(p_i^*(t) + \sum_{j\in N_{c,i}} p_j^*(t)\right).$$
Here, $p_i^d(t+1) \neq p_i^*$, $i \in (\beta)$ (if $N_{c,i} \cap (\alpha) \neq \mathbb{0}$ or $N_{c,i} \cap (\gamma) \neq \mathbb{0}$) indicating divergence from the equilibrium state. Equation (25) strives to achieve the identical incremental cost which is not possible with constrained equilibrium values in (16), resulting in infeasible ED problem.

The SDMPC technique is implemented individually on each power-node, so the size of network does not affect the processing time of the algorithm. The control employs an improved technique of calculating the desired values to provide the fast convergence to the equilibrium point. The decoupling

technique enables the implementation of the control to generic network topologies. While, the $\mathbb{A}_{\mathbb{C}}$ forces the power-nodes to follow the power production constraints and achieve the solution in (16) and (17). The design of $\mathbb{A}_{\text{SDMPC}}$ together with the terminal constraints in $\mathbb{F}_i$ results in asymptotic convergence. The analytical convergence proof is provided in the following Section.

IV. Stability Analysis

The stability of the proposed control scheme is analysed in two portions: first the convergence of desired values to the global optimum point is analysed with the help of terminal constraints, followed by the convergence of the cost function.

To show the stability of the desired states, the dynamics of the system are linearised. Calculation of desired power introduced in (25), together with terminal constraints in (27) and (28), provide asymptotic convergence to equilibrium point. While the convergence of the cost function is proved using the total cost of the network as a Lyapunov Function.

A. Convergence of terminal Constraints

We start with linearising (20), considering a large value of virtual susceptance (b_v) that results in a small phase difference $\left(\Delta\theta_i - \Delta\theta_{v,i}\right)$, for the rated value of power injection. This implies that $\sin\left(\Delta\theta_i - \Delta\theta_{v,i}\right) \approx \left(\Delta\theta_i - \Delta\theta_{v,i}\right)$. So, the power injection of a power-node is given by:

$$p_i(t) = v_i v_v b_{v,i}\left(\Delta\theta_i(t) - \Delta\theta_{v,i}(t)\right).$$

Now, linearising (33) and rewriting in vector form to represent the complete network. Also, using the assumption that the voltage of power-node and virtual-nodes is $1pu$:

$$\Delta\theta_v(t+1) = \Delta\theta^{op}(1|t) - \frac{1}{b_v}P(t). \tag{37}$$

Now, writing (30) in matrix form:

$$P^d(k|t) = \mathbb{K}P^a(k|t). \tag{38}$$

where, $\mathbb{K} = \left(\mathfrak{D}\left(C\left(A + I_{n_P}\right)C^{-1}\mathbb{1}_n\right)\right)^{-1}\left(A + I_{n_P}\right)$. The application of matrix $\mathbb{K}$ in (38) would drive the desired power to an equilibrium point. The matrix $\mathbb{K}$ possess a single eigenvalue at unit circle since the equilibrium power $P^* \neq \mathbb{0}_{n_P}$. To show the asymptotic convergence, we apply the matrix $\mathbb{K}$ on the difference $P^a(k|t) - P^*$. From Remark 3, the equilibrium value of power can be represented as $P^* = \tilde{\delta}^* C^{-1}\mathbb{1}_{n_P}$:

$$\mathbb{K}(P^a(k|t) - P^*) = \mathbb{K}\left(P^a(k|t) - \tilde{\delta}^* C^{-1}\mathbb{1}_{n_P}\right),$$
$$\mathbb{K}(P^a(k|t) - P^*) = \mathbb{K}C^{-1}\left(CP^a(k|t) - \tilde{\delta}^*\mathbb{1}_{n_P}\right). \tag{39}$$

Here, $CP^a(k|t) - \tilde{\delta}^*\mathbb{1}_{n_P}$ represents the error from the equilibrium point. For asymptotic convergence the eigenvalues of $\mathbb{K}C^{-1}$ should lie within the unit circle. The proof of convergence is provided with the help of the following Lemmata.

Lemma 2: Consider a matrix $R = \left[r_{ij}\right] \in \mathbb{R}^{n\times n}$, with the set of eigenvalues (λ_i), then according to the Geršgorin Disk Criteria [22]:

$$|\lambda - r_{ii}| \leq \sum_{j=1, j\neq i}^{n} |r_{ij}|. \tag{40}$$

For $r_{ii} \in \mathbb{R}_{\geq 0}$, (40) can be rewritten as:

$$|\lambda| \leq |r_{ii}| + \sum_{j=1, j\neq i}^{n} |r_{ij}|. \tag{41}$$

Equation (41) is a special case of (40), with non-negative diagonal elements.

Lemma 3: Consider a matrix $R = \left[r_{ij}\right] \in \mathbb{R}_{\geq 0}^{n\times n}$, such that eigenvalues of $\mathfrak{D}(R\mathbb{1}_n)$ lie within the unit circle, then the eigenvalues (λ_i) of R would be within the unit circle $(|\lambda_i| < 1)$.

Proof: $R\mathbb{1}_n$ represents the row-sum of R and the eigenvalues of $\mathfrak{D}(R\mathbb{1}_n)$ are equal to its diagonal elements, which are less than one. Since all the elements of R, $r_{ij} \geq 0$ and according to (41) the eigenvalues are less than or equal to the absolute row-sum of a matrix, so $|\lambda_i| < 1$.■

Lemma 4: The eigenvalues (λ_i) of $\mathbb{K}C^{-1} = \left(\mathfrak{D}\left(C\left(A + I_{n_P}\right)C^{-1}\mathbb{1}_{n_P}\right)\right)^{-1}\left(A + I_{n_P}\right)C^{-1}$, where $C = \mathfrak{D}(c_i) \in \mathbb{R}^{n_P\times n_P}$, lie with the unit circle, provided that $c_i > 1$.

Proof: Since C is a diagonal matrix so:

$$\mathbb{K}C^{-1} = C^{-1}\left(\mathfrak{D}\left(\left(A + I_{n_P}\right)C^{-1}\mathbb{1}_{n_P}\right)\right)^{-1}\left(A + I_{n_P}\right)C^{-1}.$$

Since, all the elements of $\mathbb{K}C^{-1}$ are greater than zero, we use Lemma 3:

$$\mathfrak{D}(\mathbb{K}C^{-1}\mathbb{1}_n) = \mathfrak{D}\begin{pmatrix} C^{-1}\left(\mathfrak{D}\left(\left(A + I_{n_P}\right)C^{-1}\mathbb{1}_{n_P}\right)\right)^{-1} \\ \left(A + I_{n_P}\right)C^{-1}\mathbb{1}_{n_P} \end{pmatrix},$$
$$= C^{-1}\left(\mathfrak{D}\left(\left(A + I_{n_P}\right)C^{-1}\mathbb{1}_{n_P}\right)\right)^{-1}\mathfrak{D}\left(\left(A + I_{n_P}\right)C^{-1}\mathbb{1}_{n_P}\right),$$
$$= C^{-1}. \tag{42}$$

Then C^{-1} is a diagonal matrix and $(c_i)^{-1} < 1$ implies that $|\lambda_i| < 1$.■

Equation (39) together with Lemma 4 provides the convergence proof of desired states to the global equilibrium point of the network.

Theorem I: Consider the power graph $\mathbb{G}$, with dynamics of the power-nodes in (5) and (6). The terminal constraints of $\mathbb{F}_i$ in (27) and (28), result in asymptotic convergence to equilibrium point defined in (9) and (10).

Proof: From (27) and (32):

$$P^{op}\left(\mathcal{N}_p|t\right) = P^p\left(\mathcal{N}_p|t\right) = P^d\left(\mathcal{N}_p|t\right).$$

Using (37):

$$P^{op}\left(\mathcal{N}_p|t\right) = \mathbb{K}P^a\left(\mathcal{N}_p|t\right). \tag{43}$$

Now, if we use the assumption for a while, that $\chi_i^a(k|t+1) = \chi_i^{op}(k+1|t)$, then the terminal value of assumed power would be:

$$P^a\left(\mathcal{N}_p - 1|t+1\right) = P^{op}\left(\mathcal{N}_p|t\right). \tag{44}$$

Now, using (28), (35) and (43):

$$P^a\left(\mathcal{N}_p|t+1\right) = \mathbb{K}P^a\left(\mathcal{N}_p|t\right). \tag{45}$$

Using Lemma 4, (45) would result in asymptotic convergence of terminal states to equilibrium.

However, it remains to prove that terminal values of assumed power $P^a\left(\mathcal{N}_p|t+1\right) \to P^{op}\left(\mathcal{N}_p|t\right)$. Since, $\theta_{v,i}$ and b_v do not represent the exact equivalent of MG at each power-node, this may result in: $p_i^a(0|t+1) = p(t) \neq p_i^{op}(1|t)$, as $\theta_{v,i}(t+1)$ may not equal the $\theta_{v,i}(t)$. Thus, the assumed trajectories $\chi_i^a(k|t+1)$ may not equal the optimum trajectories $\chi_i^{op}(k+1|t)$ within a given iteration. Now, representing the assumed trajectories in terms of optimum trajectories and $\theta_{v,i}(t+1)$ in terms of $\theta_{v,i}(t)$:

$$\chi_i^a(k|t+1) = \overline{\chi_i^a}(k|t+1) + \chi_i^{a\Delta}(k|t+1), \quad (46)$$

$$\Delta\theta_{v,i}(t+1) = \theta_{v,i}(t) + \theta_{\Delta v,i}(t+1). \quad (47)$$

Here, $\overline{\chi_i^a}$ follows the optimum trajectories; $\overline{\chi_i^a}(k|t+1) = \chi_i^{op}(k+1|t)$, while the $\chi_i^{a\Delta} = [\Delta\theta_i^{a\Delta} \quad \Delta\omega_i^{a\Delta} \quad p_i^{a\Delta}]^T$ represents the deviation from the optimum trajectories. Similarly, $\theta_{\Delta v,i}(t+1)$ represents the deviation in virtual phase at successive iterations. Now, from (32) we have:

$$\Delta\theta_i^{op}(1|t) = \theta_{v,i}(t) + \frac{1}{b_v}p_i^{op}(1|t). \quad (48)$$

So, (37) becomes:

$$\Delta\theta_v(t+1) = \theta_v(t) - \frac{1}{b_v}\big(P(t) - P^{op}(1|t)\big). \quad (49)$$

Comparing (47) and (49); $\theta_{\Delta v}(t+1) = -\frac{1}{b_v}\big(P(t) - P^{op}(1|t)\big)$.

Now, the trajectories for both $\overline{\chi_i^a}$ and $\chi_i^{a\Delta}$ would be formed as follows:

$\overline{\chi_i^a}(0|t+1) = \chi_i^{op}(1|t)$,

$\overline{\chi_i^a}(k+1|t+1) = f\left(\overline{\chi_i^a}(k|t+1), \Delta\theta_{v,i}(t), u_i^a(k+1|t)\right)$,

for $k = 0,1,\dots,\mathcal{N}_p - 2$.

Note that above equations would provide the same result as, $\overline{\chi_i^a}(k|t+1) = \chi_i^{op}(k+1|t)$. While, the terminal values of $\overline{\chi^a}$ can be found using (27), (28) and (32):

$$\overline{\chi^a}\big(\mathcal{N}_p|t+1\big) = \overline{\chi^a}\big(\mathcal{N}_p - 1|t+1\big) = \chi^{op}\big(\mathcal{N}_p|t\big). \quad (50)$$

For $\chi_i^{a\Delta}$ we have:

$$\chi_i^{a\Delta}(0|t+1) = [0 \quad 0 \quad p_i^{a\Delta}(0|t+1)],$$

$$\chi_i^{a\Delta}(k+1|t+1) = f\big(\chi_i^{a\Delta}(k|t+1), \theta_{\Delta v,i}(t+1), 0\big). \quad (51)$$

In equation (51), $\Delta\theta_i^{a\Delta}(0|t+1)$ & $\Delta\omega_i^{a\Delta}(0|t+1)$ are zero. Note that the control input in (51) is also zero while, $p_i^{a\Delta}(0|t+1) = p(t) - p_i^{op}(1|t) = b_v\left(\Delta\theta_i^{a\Delta}(0|t+1) - \theta_{\Delta v,i}(t+1)\right)$.

Remark 5: The natural response of $f\big(\chi_i^{a\Delta}(k|t+1), \theta_{\Delta v,i}(t+1), 0\big)$ with zero input and initial conditions, $\chi_i^{a\Delta}(0|t+1) = [0 \quad 0 \quad p_i^{a\Delta}(0|t+1)]^T$, is: $\chi_i^{a\Delta}(k|t+1) \to [\theta_{\Delta v,i}(t+1) \quad 0 \quad 0]^T$ for $k \geq 3$.

The result in Remark 5 supports the assumption in (44). Since, the terminal value of $p_i^{a\Delta}$ asymptotically converges to zero, this implies that the terminal value; $P^a \to \overline{P^a} = P^{op}$, completing the proof. ■

B. Convergence of Cost Function

To show the convergence of the cost function, we consider an optimum value of cost function $J_i^*(t)$ and compare it with the suboptimal value of cost function. Now the optimum value is given by:

$$J_i^*(t) = J_i^*\left(\chi_i^{op}(:|t), u_i^{op}(:|t), \chi_i^a(:|t), \Delta\theta_i^d(:|t)\right), \quad (52)$$

$$J_i^*(t) = \sum_{k=1}^{\mathcal{N}_p} l_i\left(\chi_i^{op}(k|t), u_i^{op}(k|t), \chi_i^a(k|t), \Delta\theta_i^d(k|t)\right). \quad (53)$$

Now, according to [22],[23], the feasible solution of $\mathbb{F}_i$ is given by:

$$\left(\chi_i^p(:|t), u_i^p(:|t)\right) = \left(\chi_i^a(:|t), u_i^a(:|t)\right). \quad (54)$$

Equation (54), represents the feasible solution which may not be an optimum solution of $\mathbb{F}_i$.

Theorem 2: For the power graph $\mathbb{G}$, with dynamics of the power-nodes in (5) and (6) and satisfying Theorem 1, the cost function of $\mathbb{F}_i$ in (29) would converge asymptotically satisfying:

$$J_i^*(t+1) - J_i^*(t) \leq -l_i\left(\chi_i^{op}(1|t), u_i^{op}(1|t), \chi_i^a(1|t), \Delta\theta_i^d(1|t)\right) - \sum_{k=2}^{\mathcal{N}_p} ||\chi_i^{op}(k|t) - \chi_i^a(k|t)||.$$

Proof: Comparing the optimum cost function in (53) with sub-optimum cost function obtained from (54), at time $t = t + 1$:

$$J_i^*(t+1) \leq J_i\left(\chi_i^a(:|t+1), u_i^a(:|t+1), \chi_i^a(:|t+1), \Delta\theta_i^d(:|t+1)\right),$$

$$\leq \sum_{k=1}^{\mathcal{N}_p} l_i\left(\chi_i^a(:|t+1), u_i^a(:|t+1), \chi_i^a(:|t+1), \Delta\theta_i^d(:|t+1)\right).$$

From the terminal constraints in (27), (28) and sub-optimal solution in (54):

$$l_i\left(\chi_i^a\big(\mathcal{N}_p|t+1\big), u_i^a\big(\mathcal{N}_p|t+1\big), \chi_i^a\big(\mathcal{N}_p|t+1\big), \Delta\theta_i^d\big(\mathcal{N}_p|t+1\big)\right) = 0.$$

So,

$$J_i^*(t+1) \leq \sum_{k=1}^{\mathcal{N}_p-1} l_i\left(\chi_i^a(k|t+1), u_i^a(k|t+1), \chi_i^a(k|t+1), \Delta\theta_i^d(k|t+1)\right).$$

Now, from Theorem 1, $\chi_i^{a\Delta}(k|t+1) = 0$ for $t \geq t$; results in $\chi_i^a(k|t+1) = \chi_i^{op}(k+1|t)$ and

$$J_i^*(t+1) \leq \sum_{k=1}^{\mathcal{N}_p-1} l_i\left(\chi_i^{op}(k+1|t), u_i^{op}(k+1|t), \chi_i^{op}(k+1|t), \Delta\theta_i^d(k+1|t)\right),$$

$$J_i^*(t+1) \leq \sum_{k=2}^{\mathcal{N}_p} l_i\left(\chi_i^{op}(k|t), u_i^{op}(k|t), \chi_i^{op}(k|t), \Delta\theta_i^d(k|t)\right). \quad (55)$$

Subtracting (55) and (53):

$$J_i^*(t+1) - J_i^*(t) \leq \sum_{k=2}^{\mathcal{N}_p} l_i\left(\chi_i^{op}(k|t), u_i^{op}(k|t), \chi_i^{op}(k|t), \Delta\theta_i^d(k|t)\right) - \sum_{k=1}^{\mathcal{N}_p} l_i\left(\chi_i^{op}(k|t), u_i^{op}(k|t), \chi_i^a(k|t), \Delta\theta_i^d(k|t)\right),$$

$$\leq \sum_{k=2}^{\mathcal{N}_p} ||\chi_i^{op}(k|t) - \chi_i^{op}(k|t)|| + ||\Delta\theta_i^{op}(k|t) - \Delta\theta_i^d(k|t)|| + ||\Delta\omega_i^{op}(k|t)|| - \sum_{k=1}^{\mathcal{N}_p} ||\chi_i^{op}(k|t) - \chi_i^a(k|t)|| + ||\Delta\theta_i^{op}(k|t) - \Delta\theta_i^d(k|t)|| + ||\Delta\omega_i^{op}(k|t)||,$$

$$\leq -l_i\left(\chi_i^{op}(1|t), u_i^{op}(1|t), \chi_i^a(1|t), \Delta\theta_i^d(1|t)\right) - \sum_{k=2}^{\mathcal{N}_p} ||\chi_i^{op}(k|t) - \chi_i^a(k|t)||. \quad (56)$$

From the definition of the cost function in (29), $l_i(\cdot) \geq 0$ and $||\chi_i^{op}(k|t) - \chi_i^a(k|t)|| \geq 0$, completing the proof. ■

Theorem 3: For the power graph $\mathbb{G}$, with the dynamics of power-nodes in (5) and satisfying Theorem 1, the total cost of the network; $\mathbb{J}^*(t) = \sum_{i=1}^{N_P} J_i^*(t)$, would converge asymptotically and satisfy:

$$\mathbb{J}^*(t+1) - \mathbb{J}^*(t) \leq -\sum_{i=1}^{N_P} l_i\left(\chi_i^{op}(1|t), u_i^{op}(1|t), \chi_i^a(1|t), \Delta\theta_i^d(1|t)\right) - \sum_{i=1}^{N_P}\sum_{k=2}^{\mathcal{N}_p} ||\chi_i^{op}(k|t) - \chi_i^a(k|t)||. \quad (57)$$

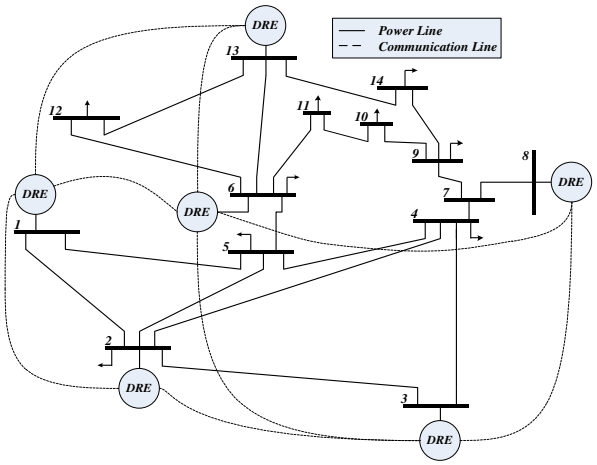

Figure 2. IEEE 14-Bus Test System

Proof: The summation of (56) for the complete set of power-nodes provides (57).■

Equation (39) together with the results in Lemma 4 provides the proof for asymptotic convergence of desired state values, provided that the cost rate $c_i > 1$. The stability of the terminal states provided in Theorem 1 is based on equality based terminal constraints in $\mathbb{F}_i$. The deviation of assumed trajectories from optimum state trajectories is analysed, which is caused by the change in virtual phase angle. However, the terminal values of assumed trajectories approach the optimum trajectories with sufficiently large values of prediction horizon $(\mathcal{N}_p > 3)$, as discussed in Remark 5. Theorem 2 provides the convergence proof of the cost function for individual power nodes while, the convergence of the cost for entire network is presented in Theorem 3.

V. Performance Validation

The proposed control is simulated on an IEEE 14-Bus System and the performance is compared with DAI control. As shown in Figure 2, six DRES based power-nodes are used in the system $(n_P = 6)$, so, the resulting set of power nodes is; $N_P = \{n_1 \quad n_2 \quad n_3 \quad n_6 \quad n_8 \quad n_{13}\}$. The performance of the proposed control strategy is analysed using two test cases.

- Case-I demonstrates the fast convergence and ability of proposed control to anticipate the upcoming planned changes. Both planned and unplanned abrupt changes, as well as continuous fluctuations in power demand are introduced to test the performance of SDMPC.
- Case-II represents the performance of the proposed control in presence of production constraints to provide the constrained ED solution.

A. Cases-I

This case represents the response of the proposed control to different types of disturbances and fluctuations\changes in the system while, assuming sufficiently large production limits $(\mathbb{0}_{n_P} \leq P \leq \infty\mathbb{1}_{n_P})$. Abrupt changes are introduced at simulation times of 1 second and 9 seconds while, continuous fluctuations in power demand are introduced between the simulation time of 3.5 seconds to 8 seconds. The disturbances cause the deviation in frequency and optimum production in the network. An unplanned change at 1 second is caused by a sudden decrease in power demand, while the abrupt change at 9 seconds is a planned disturbance and all the power-nodes in the network have prior information of the disturbance. The simulation time of 9 seconds is considered as the start of peak-hours, where the production cost rate (c_i) of all the power-nodes increases abruptly and not uniformly, disturbing the consensus to identical incremental cost.

Figure 3 represents the convergence to identical incremental cost with the proposed control scheme. The largest deviation in ED point (and frequency) is caused by the unplanned abrupt change at 1 second however, the fluctuations in incremental cost are damped within 0.4 seconds. The control actively maintains the consensus for ED for varying power demand between 3.5 seconds to 8 seconds. Since the disturbance at 9 seconds is a planned disturbance, each node in Figure 3, anticipates the change in cost before 9 seconds resulting in a relatively smooth transition to peak hours. Figure 4 represents the frequency deviation of the individual power nodes. The maximum frequency deviation takes place at 1 second due to the unplanned abrupt change in power demand. However, the amplitude of deviation in frequency is less than 0.1 (rad/sec) which is well within the acceptable limits for the system.

Figures 5 and 6 respectively represent the incremental cost and frequency deviation with DAI control schemes. As shown in Figure 5 the system hardly achieves the consensus to identical incremental cost after the disturbance at 1 second, illustrating the slow response of the control. However, in Figure 6 the control provides excellent frequency regulation with minimal deviations.

The proposed control scheme outperforms the DAI control in terms of fast convergence to maintain the ED. Since the power networks frequently undergoes fluctuations in power demand, the slow nature of DAI would fail to provide the ED resulting in increased production cost and degraded power quality. The proposed control scheme does exhibit relatively greater deviation in frequency, however the amplitude of the deviations is well within the acceptable limits.

B. Cases-II

This case represents the convergence to identical incremental cost in the presence of production constraints. The production constraints used in the paper are; $P^{min} = \mathbb{0}_6$ and $P^{max} = [0.60 \quad 0.85 \quad 1.30 \quad 0.70 \quad 0.80 \quad 0.62]^T(pu)$. The simulation starts at equilibrium state, with equilibrium power (P^*) lying well within the production limits $P^{min} < P^* < P^{max}$, resulting in $\delta^* = \bar{\delta}^*$. The power demand in the system is increased linearly after the simulation time of 1 second resulting in increased power injection by the individual power-nodes. Consequently, the ED solution approaches the maximum production limits for the power-nodes; n_1 at simulation time of 1.63 seconds and n_{13} at the simulation time of 3.05 seconds.

The proposed control scheme successfully achieves the constrained ED solution defined in (16) and (17). Figure 7 represents the actual incremental cost $(\mathrm{c_i p_i})$ of power-nodes with the proposed control scheme. The incremental cost of nodes n_1 and n_{13} saturates at $c_1 p_1^{max}$ and $c_{13} p_{13}^{max}$, while the

incremental cost of the remaining nodes converge to an identical value; $c_2 p_2 = c_3 p_3 = c_6 p_6 = c_8 p_8 = \tilde{\delta}^*$. Figure 8 represents

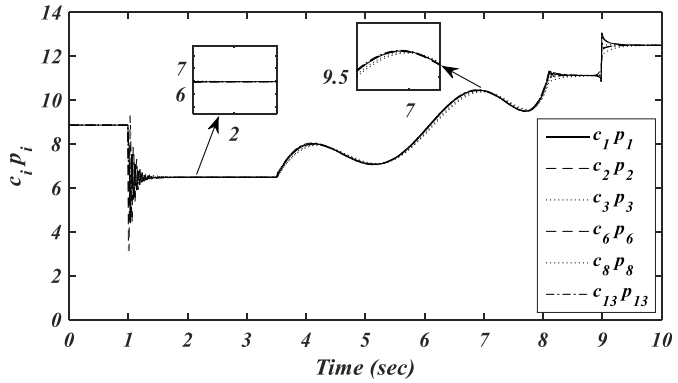

Figure 3. SDMPC: Identical Incremental Cost $(c_i p_i)$

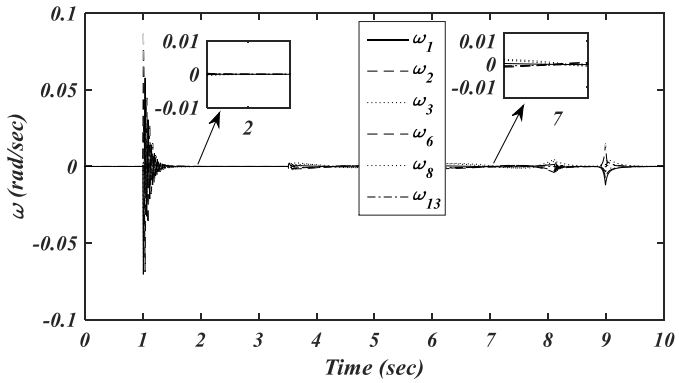

Figure 4. SDMPC: Frequencies deviation $(\Delta\omega_i)$

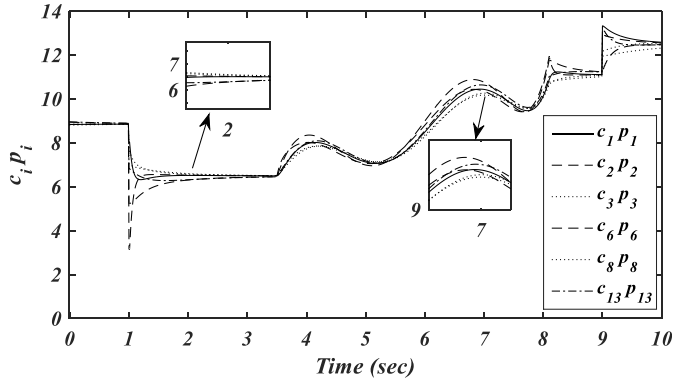

Figure 5. DAI control: Identical Incremental Cost $(c_i p_i)$

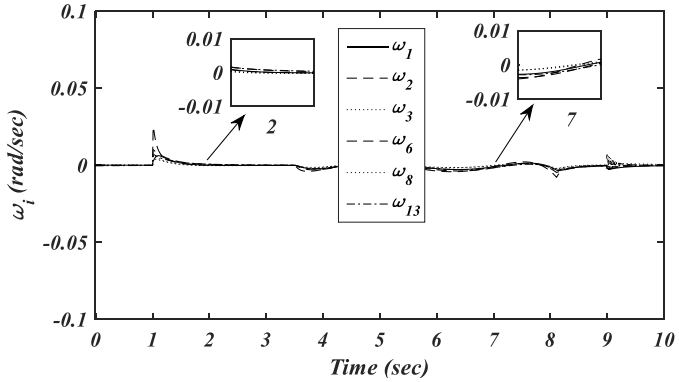

Figure 6. DAI control: Frequencies deviation $(\Delta\omega_i)$

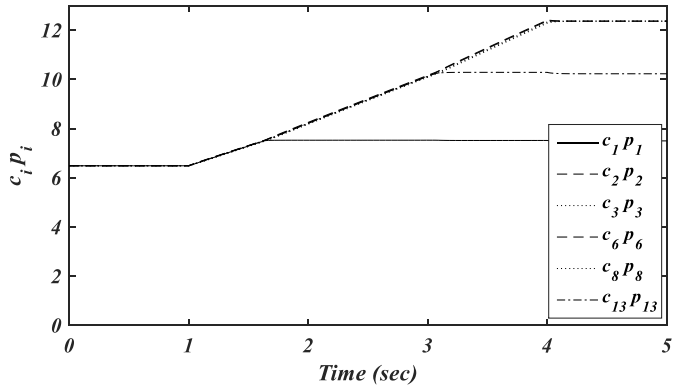

Figure 7. SDMPC: Identical Incremental Cost $(c_i p_i)$, with Actual Power (p_i)

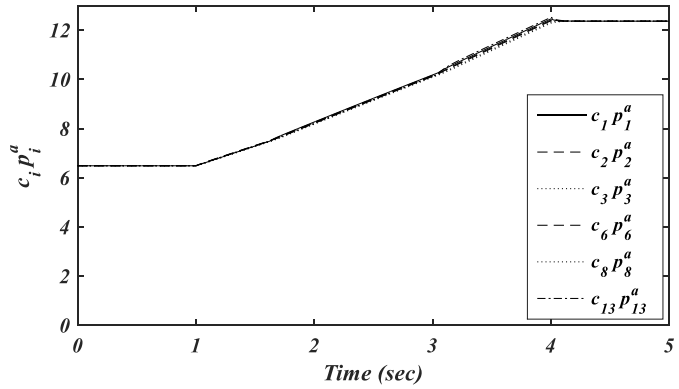

Figure 8. SDMPC: Identical Incremental Cost $(c_i p_i^a)$, with Assumed Power (p_i^a)

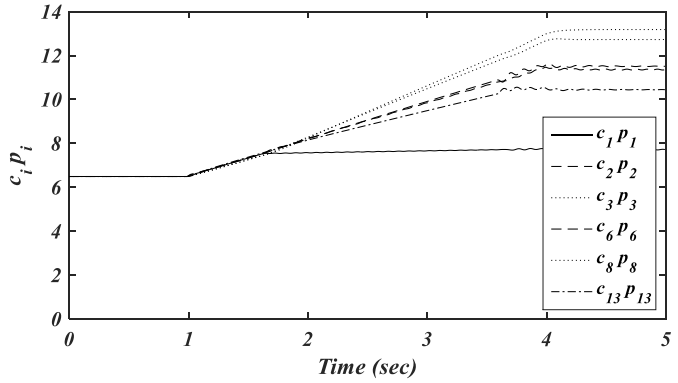

Figure 9. DAI control: Identical Incremental Cost $(c_i p_i)$

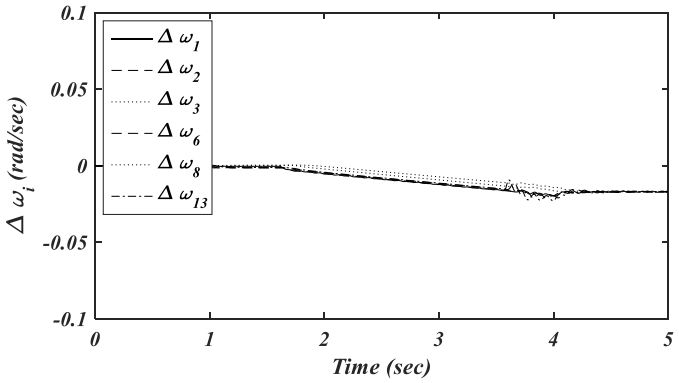

Figure 10. DAI control: Frequencies deviation $(\Delta\omega_i)$

the convergence of all the power-nodes to constrained optimum cost with assumed power $\left(CP^{a} = \tilde{\delta}^{*}\mathbb{1}_{n_P}\right)$, as discussed in Remark 3.

Figure 9 represents the performance of DAI control scheme in presence of production constraints. The control diverges as soon as the single node (n_1) reaches its maximum production limit and fails to maintain the ED in the system. Figure 10 illustrates that the control also fails to achieve the frequency regulation in the system after simulation time of 1.63 seconds.

In summary, this Section has demonstrated the value of the proposed approach in that:

- The proposed SDMPC provides active frequency regulation and fast convergence to ED, in the presence of abrupt disturbances as well as continuous fluctuations in the power demand. Whereas, DAI control possesses slow convergence and fails to converge in presence of fluctuating power demand, resulting in increased production cost.
- The response of SDMPC is particularly better in the case of planned disturbances, employing the inherent capability of MPC to anticipate the future changes.
- The proposed control successfully handles the production constraints and achieves the constrained ED solution whereas, DAI based control becomes unstable when a single power-node saturates at its maximum production limit.

VI. CONCLUSIONS

This paper addresses the frequency regulation and ED of autonomous MG. The paper presents a technique to implement a DMPC based *secondary* control technique to the nonlinear coupled dynamics of MG. The concept of a virtual-node is introduced to create a decoupled system with known parameters, enabling the construction of state predictions and implementation to generic network topologies. The control benefits from the inherent capabilities of DMPC such as; fast convergence and anticipation of upcoming planned changes, to effectively comply with the control requirements of low inertia MG. Whereas, distributed integral based control fails to converge to an ED solution in the presence of fluctuating power demands, resulting in increased production cost. Considering a practical scenario of volatile production capacity of DRES, the Constraints Handling Algorithm is proposed to achieve the constrained ED solution. While, the contemporary control solutions become unstable as a single DRES node saturates at its extreme production limit. The stability of the control is ensured with the help of terminal constraints and convergence is proved using the total cost of the network as a Lyapunov Candidate Function. For future work the presented control strategy can be extended to provide the voltage and reactive power sharing at *secondary* control simultaneously, with frequency regulation and ED.

VII. REFERENCES

[1] H. Xing; Z. Lin; Minyue Fu; B. F. Hobbs (2017, July.). Distributed algorithm for dynamic economic power dispatch with energy storage in smart grids. *IET Control Theory & Applications,* vol. 11, issue. 11, doi: 10.1049/iet-cta.2016.1389.

[2] J. Lai; Xiaoqing Lu; Z. Dong; Ruo-li Tang (2019, July). Robustness-oriented distributed cooperative control for ac microgrids under complex environments. *IET Control Theory & Applications,* vol. 13, issue. 10, doi: 10.1049/iet-cta.2018.5698.

[3] J. Lianos; J. Gomez; D. Saez; D. Olivares; J. S. Porco (2019, Sept). Economic Dispatch by Secondary Distributed Control in Microgrids. 2019 21st European Conference on Power Electronics and Applications (EPE 19 ECCE Europe), Genova, Italy, doi: 10.23919/EPE.2019.8915499.

[4] M. Yazdanian; A. M. Sani (2014, Aug). Distributed Control Techniques in Microgrids. *IEEE Transactions on Smart Grid,* vol. 5, issue 6, doi: 10.1109/TSG.2014.2337838.

[5] J. Schiffer; F. Dorfler; E. Fridman (2017, June). "Robustness of distributed averaging control in power systems: Time delays & dynamic communication topology". *Automatica,* vol. 80, doi: 10.1016/j.automatica.2017.02.040.

[6] F. Dorfler; J. W. Simpson-Porce; F. Bullo (2016, Sept). Breaking the Hierarchy: Distributed Control & Economic Optimality in Microgrids *IEEE Transaction on Control of Network System,* vol.3, issue. 3 doi: 10.1109/TCNS.2015.2459391.

[7] F. Mehmood, B. Khan, S. M. Ali, J. A. Rossiter (2019, Nov). Distributed Model Predictive based Secondary Control for Economic Production and Frequency Regulation of Microgrid. *IET Control Theory & Applications,* vol. 13, issue 17, doi: 10.1049/iet-cta.2018.6226.

[8] X. Y. Jiang; Chuan He; K. Jermsittiparsert (2019, Nov). Online optimal stationary reference frame controller for inverter interfaced distributed generation in a microgrid system. *Energy Reports,* vol. 6, doi: 10.1016/j.egyr.2019.12.016.

[9] B. K. Poolla; D. Groß; F. Dörfler (2019, July). Placement and Implementation of Grid-Forming and Grid-Following Virtual Inertia and Fast Frequency Response. *IEEE Transactions on Power Systems,* vol. 34, Issue 4, doi: 10.1109/TPWRS.2019.2892290.

[10] R. Zamora, A.K. Srivastava (2018). "Multi-Layer Architecture for Voltage and Frequency Control in Networked Microgrids", *IEEE Transactions on Smart Grid,* vol: 9, issue 3, doi:10.1109/TSG.2016.2606460.

[11] A. Mohammad, S. S. Refaat, S. Bayhan, H. Abu-Rub (2019, Jun). "AC Microgrid Control and Management Strategies: Evaluation and Review", *IEEE Power Electronics Magazine,* doi: 10.1109/MPEL.2019.2910292.

[12] H. R. Baghaee; A. Parizad; M. Shafie-Khan; P. Siano (2019, Oct). Robust Primary Control of Microgrids for Parametric and Topological Uncertainties: A Quest for Resilience. 2019 23rd International Conference on Mechatronics Technology (ICMT), Salerno Italy, doi: 10.1109/ICMECT.2019.8932113.

[13] X. Wang, H. Zhang, Changxi Li (2016, Nov). "Distributed finite-time cooperative control of droop-controlled microgrids under switching topology", *IET Renewable Power Gneration,* vol. 11, issue 5, doi: 10.1049/iet-rpg.2016.0526.

[14] Y. Khayat, Q. Shafiee, R. Heydari, M. Naderi (2019, Nov). "On the Secondary Control Architecture of AC Microgrids: An Overview", *IEEE Transactions on Power Electronics,* doi: 10.1109/TPEL.2019.2951694.

[15] C. Zhao; E. Mallada; F. Dorfler (2015, July) "Distributed Frequency Control for Stability and Economic Dispatch in Power Networks", American Control Conference, Chicago IL, USA, doi: 10.1109/ACC.2015.7171085.

[16] P. T. de Godoy; P. Poloni; A. B. de Almeida; D. Marujo (2019, Sept). Centralized Secondary Control Assessment of Microgrids with Battery and Diesel Generator. 2019 IEEE PES Innovative Smart Grid Technologies Conference - Latin America (ISGT Latin America), Gramado, Brazil, doi: 10.1109/ISGT-LA.2019.8895294.

[17] Z. Li; Z. Cheng; J.J. Liang; Jikai Si; L. Dong (2019, Oct). Distributed Event-triggered Secondary Control for Economic Dispatch and Frequency Restoration Control of Droop-controlled AC Microgrids. I*EEE Transactions on Sustainable Energy,* doi: 10.1109/TSTE.2019.2946740.

[18] Kaihua Xi; Johan L.A; Dubbeldam (2018, June), "Power-Imbalance Allocation Control of Power Systems-Secondary Frequency Control", *Automatica*, vol. 92, doi: 10.1016/j.automatica.2018.02.019.

[19] Ji Xiang; Yu Wang; Yanjun Li; Wei We (2016, Dec) Stability and steady-state analysis of distributed cooperative droop controlled DC microgrids, *IET Control Theory & Applications,* vol. 10, issue 18, doi: 10.1049/iet-cta.2016.0496.

[20] S. Porco; John W.; F. Dörfler; F. Bullo, (2013, Feb). Synchronization and power sharing for droop-controlled inverters in islanded microgrids. *Automatica*, doi: 10.1016/j.automatica.2013.05.018.

[21] G. Magdy; G. Shabib; A. A. Elbaset, Y. Mitani (2019, July). Renewable power systems dynamic security using a new coordination of frequency control strategy based on virtual synchronous generator and digital frequency protection. *International Journal of Electrical Power & Energy Systems,* vol. 109, doi: 10.1016/j.ijepes.2019.02.007.

[22] Y. Zheng; S. Eben Li; K. Li; F. Borrelli (2017, Aug). Distributed Model Predictive Control for Heterogenous Vehicle Platoons under Unidirectional Topologies, *IEEE Transactions on Control Systems Technology* vol. 25 , issue. 3, doi: 10.1109/TCST.2016.2594588.

[23] W. Dunbar and D. Caveney (2012, Mar). Distributed receding horizon control of vehicle platoons: Stability and string stability. *IEEE Trans. Autom. Control,* vol. 57, issue 3, doi: 10.1109/TAC.2011.2159651.